AFRL-AFOSR-VA-TR-2015-0385

(DARPA) Q-BOOSTED OPTOMECHANICAL RESONATORS

Clark Nguyen
REGENTS OF THE UNIVERSITY OF CALIFORNIA THE

11/18/2015
Final Report

Air Force Research Laboratory
AF Office Of Scientific Research (AFOSR)/ RTB1
Arlington, Virginia 22203
Air Force Materiel Command

REPORT DOCUMENTATION PAGE

Form Approved
OMB No. 0704-0188

PLEASE DO NOT RETURN YOUR FORM TO THE ABOVE ORGANIZATION.

1. REPORT DATE *(DD-MM-YYYY)*	2. REPORT TYPE	3. DATES COVERED *(From - To)*
15-09-2015	Final Technical Report	7/1/10 to 6/30/15

4. TITLE AND SUBTITLE
Q-Boosted Optomechanical Resonators

5a. CONTRACT NUMBER

5b. GRANT NUMBER
FA9550-10-1-0293

5c. PROGRAM ELEMENT NUMBER

6. AUTHOR(S)
Clark T.-C. Nguyen

5d. PROJECT NUMBER

5e. TASK NUMBER

5f. WORK UNIT NUMBER

7. PERFORMING ORGANIZATION NAME(S) AND ADDRESS(ES)
Dept. of Electrical Engineering & Computer Sciences
University of California at Berkeley
Berkeley, CA 94720

8. PERFORMING ORGANIZATION REPORT NUMBER

9. SPONSORING/MONITORING AGENCY NAME(S) AND ADDRESS(ES)
DOD Advanced Research Projects Agency (DARPA)
675 North Randolph Street
Arlington, VA
Monitor: AFOSR

10. SPONSOR/MONITOR'S ACRONYM(S)
DARPA/MTO and AFOSR

11. SPONSOR/MONITOR'S REPORT NUMBER(S)

12. DISTRIBUTION/AVAILABILITY STATEMENT
DISTRIBUTION A

13. SUPPLEMENTARY NOTES

14. ABSTRACT

This grant set out to prove that heterogeneous combination of multiple materials greatly im-proves optomechanical oscillator performance to point of permitting demonstration of actual re-al-world applications, such as the optical receiver that culminated this work. In this endeavor, the grant has been quite successful, as it has yielded HF to VHF optomechanical oscillators with the lowest in-class room temperature phase noise yet demonstrated. In particular, the energy sharing approach ("dubbed Q-boosting") combines polysilicon and silicon nitride materials to allow simultaneous high mechanical Qm and higher optical Qo than attainable by polysilicon material alone.

15. SUBJECT TERMS

16. SECURITY CLASSIFICATION OF:			17. LIMITATION OF ABSTRACT	18. NUMBER OF PAGES	19a. NAME OF RESPONSIBLE PERSON
a. REPORT	b. ABSTRACT	c. THIS PAGE		25	Clark T.-C. Nguyen
					19b. TELEPHONE NUMBER *(Include area code)* 510-642-6251

INSTRUCTIONS FOR COMPLETING SF 298

1. REPORT DATE. Full publication date, including day, month, if available. Must cite at least the year and be Year 2000 compliant, e.g. 30-06-1998; xx-06-1998; xx-xx-1998.

2. REPORT TYPE. State the type of report, such as final, technical, interim, memorandum, master's thesis, progress, quarterly, research, special, group study, etc.

3. DATES COVERED. Indicate the time during which the work was performed and the report was written, e.g., Jun 1997 - Jun 1998; 1-10 Jun 1996; May - Nov 1998; Nov 1998.

4. TITLE. Enter title and subtitle with volume number and part number, if applicable. On classified documents, enter the title classification in parentheses.

5a. CONTRACT NUMBER. Enter all contract numbers as they appear in the report, e.g. F33615-86-C-5169.

5b. GRANT NUMBER. Enter all grant numbers as they appear in the report, e.g. AFOSR-82-1234.

5c. PROGRAM ELEMENT NUMBER. Enter all program element numbers as they appear in the report, e.g. 61101A.

5d. PROJECT NUMBER. Enter all project numbers as they appear in the report, e.g. 1F665702D1257; ILIR.

5e. TASK NUMBER. Enter all task numbers as they appear in the report, e.g. 05; RF0330201; T4112.

5f. WORK UNIT NUMBER. Enter all work unit numbers as they appear in the report, e.g. 001; AFAPL30480105.

6. AUTHOR(S). Enter name(s) of person(s) responsible for writing the report, performing the research, or credited with the content of the report. The form of entry is the last name, first name, middle initial, and additional qualifiers separated by commas, e.g. Smith, Richard, J, Jr.

7. PERFORMING ORGANIZATION NAME(S) AND ADDRESS(ES). Self-explanatory.

8. PERFORMING ORGANIZATION REPORT NUMBER. Enter all unique alphanumeric report numbers assigned by the performing organization, e.g. BRL-1234; AFWL-TR-85-4017-Vol-21-PT-2.

9. SPONSORING/MONITORING AGENCY NAME(S) AND ADDRESS(ES). Enter the name and address of the organization(s) financially responsible for and monitoring the work.

10. SPONSOR/MONITOR'S ACRONYM(S). Enter, if available, e.g. BRL, ARDEC, NADC.

11. SPONSOR/MONITOR'S REPORT NUMBER(S). Enter report number as assigned by the sponsoring/ monitoring agency, if available, e.g. BRL-TR-829; -215.

12. DISTRIBUTION/AVAILABILITY STATEMENT. Use agency-mandated availability statements to indicate the public availability or distribution limitations of the report. If additional limitations/ restrictions or special markings are indicated, follow agency authorization procedures, e.g. RD/FRD, PROPIN, ITAR, etc. Include copyright information.

13. SUPPLEMENTARY NOTES. Enter information not included elsewhere such as: prepared in cooperation with; translation of; report supersedes; old edition number, etc.

14. ABSTRACT. A brief (approximately 200 words) factual summary of the most significant information.

15. SUBJECT TERMS. Key words or phrases identifying major concepts in the report.

16. SECURITY CLASSIFICATION. Enter security classification in accordance with security classification regulations, e.g. U, C, S, etc. If this form contains classified information, stamp classification level on the top and bottom of this page.

17. LIMITATION OF ABSTRACT. This block must be completed to assign a distribution limitation to the abstract. Enter UU (Unclassified Unlimited) or SAR (Same as Report). An entry in this block is necessary if the abstract is to be limited.

Final Report

Grant Number:	**FA9550-10-1-0293**
DARPA Program:	**BAA 09-26, Optical Radiation Cooling and Heating in Integrated Devices (ORCHID)**
Lead Organization:	**University of California at Berkeley**
Project Title:	**Q-Boosted Optomechanical Resonators**

Technical POC:	**Professor Clark T.-C. Nguyen** Department of Electrical Engineering and Computer Sciences University of California at Berkeley 574 Cory Hall, Berkeley, CA 94720-1770	
	Telephone:	(510) 642-6251
	FAX:	(510) 643-6637
	E-mail:	ctnguyen@eecs.berkeley.edu
Co-I :	**Professor Ming C. Wu, EECS**	
Administrative POC :	**Ms. Patricia Gates** Sponsored Projects Office University of California at Berkeley 2150 Shattuck Avenue, Room 313, Berkeley, CA 94704-5940	
	Telephone:	(510) 642-8109
	FAX:	(510) 642-8236
	E-mail:	spoawards@berkeley.edu

Submitted To :	**Robert Lutwak, DARPA/MTO**
	Tatjana Curcic, AFOSR
Period Covered :	**July 1, 2010 to June 30, 2015 (includes no cost extension)**
Submitted :	**Sept. 18, 2015**

Table of Contents

Bulleted Summary of Major Accomplishments Over the Entire Grant Period

- Employed an exhaustive set of experiments to identify optimal annealing conditions to maximize the Q_o of reflowed PSG OMO spoke-supported rings.
- Demonstrated an OMO attaining an anchor-loss-limited mechanical Q_m of 10,400 in vacuum that posted a best-to-date (at the time) phase noise of -102 dBc/Hz at a 1-kHz offset from a 74-MHz carrier, which at the time was more than 15 dB better than the best previously published mark [1]. While enhanced optical and mechanical Q both serve to lower the optical threshold power required for oscillation, it is the mechanical Q_m that ends up having the strongest impact on phase noise [2], much as in a traditional MEMS-based oscillator [3]. The improved phase noise performance of this OMO was on par with many conventional MEMS-based oscillators and is sufficient for the targeted chip-scale atomic clock application.
- Demonstrated a co-planar OMO comprised of attached concentric rings of polysilicon and silicon nitride that achieved a first demonstration of a mixed material optomechanical device, posting a Q_m of 22,300 at 52 MHz, which is more than 2× larger than previous single-material silicon nitride devices [4]. With this Q_m, the OMO exhibits a best-to-date phase noise of -114 dBc/Hz at 1 kHz offset from its 52-MHz carrier—a 12 dB improvement from the previous best by an OMO constructed of silicon nitride alone [4]. The key to achieving this performance is the unique mechanical *Q*-boosting design where most of the vibrational energy is stored by the high-Q_m polysilicon inner ring which in turn boosts the over-all mechanical Q_m over that of silicon nitride, all while retaining the high optical Q_o > 190,000 of silicon nitride material.
- Demonstrated a multi-material composite OMO comprised of a silicon nitride ring stacked atop a polysilicon ring in a vertically coupled fashion realized a first demonstration of a 3-D optomechanical device, allowing independent optimization of optical and mechanical properties as well as electromechanical coupling. The first rendition of this device, with lithographically defined electrode gap requiring a simpler fabrication but sacrificing electromechanical coupling, realized an 87 MHz OMO with a threshold power below one mW.

- Demonstrated a stacked-ring OMO using a process similar to previously demonstrated MEMS resonators [3] that allows definition of the electrode gap spacing by the sacrificial layer thickness, resulting in a much smaller gap and much stronger electromechanical coupling and stronger voltage-controlled electrical stiffness frequency pulling than previous such devices. The addition of the silicon nitride ring and the associated vertical couplers above the polysilicon MEMS structure requires only 2 more lithography steps atop a fairly mature and standard process flow. The measured resonance frequency as a function of bias voltage V_P for one such device yields a curve consistent with a 40 nm electrode-to-resonator gap. The observed corresponding frequency shift is almost 20 ppm/V, to be compared to the 3 ppm/V of the co-planar OMO.
- Locked an Optomechanical Voltage Controlled Oscillator (OMVCO), realized by the co-planar device of the previous section, to a microwave source to greatly improve the OMVCO's long term drift while simultaneously retaining its excellent short term characteristics. In particular, phase-locking the 9^{th} harmonic of a OMVCO at 466 MHz to an RF signal generator improved the phase noise by 85dB at 1 Hz offset, while maintaining a phase noise of -140 dBc/Hz at offsets >50 kHz; yielding a reduction in Allan deviation by 20 dB.
- Utilized the *Q*-boosted OMO to realize a first super-regenerative optical receiver that detects on-off key modulated light input via the radiation-pressure gain of a self-sustained electro-opto-mechanical oscillator (EOMO), as illustrated in Figure 18. With oscillation amplitude a function of the intensity of light coupled into the oscillator, this device now allows data to be directly demodulated using only silicon-compatible materials, i.e., without the expensive III-V compound semiconductor materials often used in conventional optical receivers.

1. Project Goals

The proposed work aimed to explore methods for attaining optomechanical resonators with simultaneous high optical Q_o and high mechanical Q_M for use first as ultra-low-noise microwave oscillators for chip-scale atomic clocks and later in optical receivers. The crux of the proposed work is a mechanical circuit that allows independent optimization of the optical Q_o and mechanical Q_M of the composite resonant structure, thereby obviating the need to trade-off Q_o and Q_M that has hindered previous optomechanical resonator designs.

2. Approach & Problems To Be Addressed

Fig. 1 presents a pictorial description of the targeted optomechanical circuit that harnesses numerous innovations, including:

1) Use of a ***Q-boosting mechanically coupled array circuit*** invented by the PI [5] to raise the mechanical Q_M's of high optical Q_o, but low mechanical Q_M, resonators. In particular, as indicated in Fig. 1(a) and later in this section, materials with the highest optical Q_o's, such as CaF_2, will likely not exhibit the highest mechanical Q_M's, for which materials like silicon, diamond, or SiC, are preferred. Thus, optomechanical resonators that utilize single resonant structures must often optimize optical Q_o at the expense of mechanical Q_M. The structure of Fig. 1, on the other hand, mechanically couples several high Q_M resonators to a (potentially low-Q_M, but high

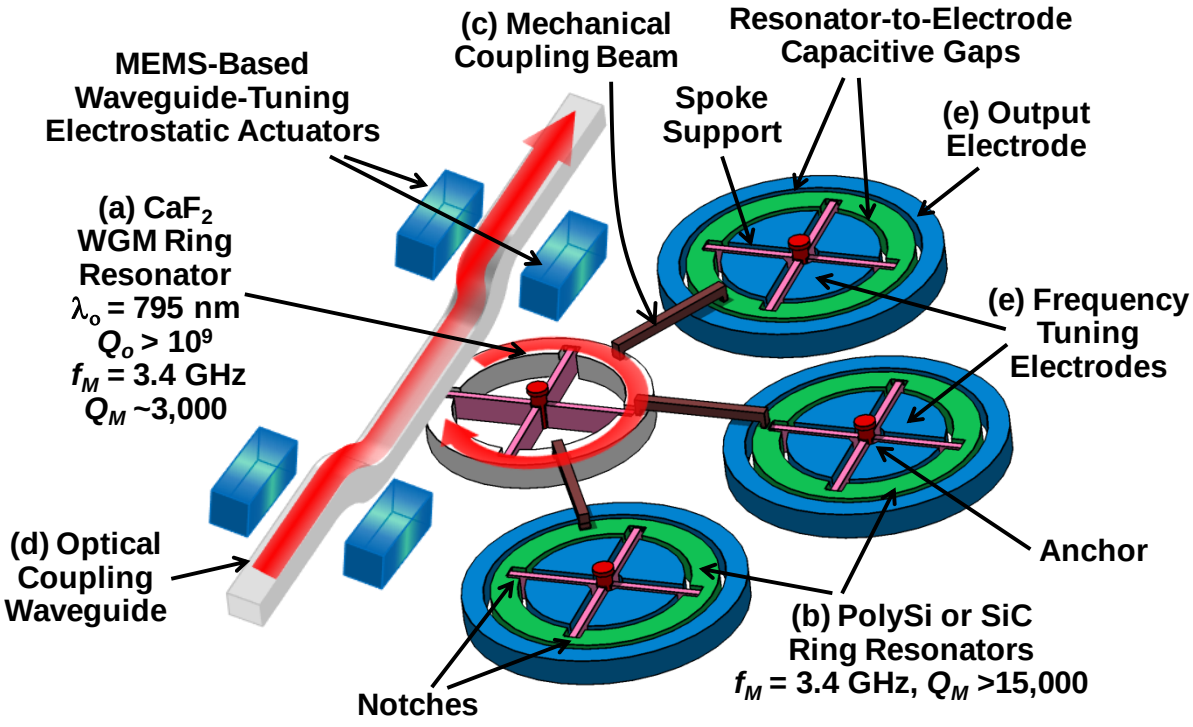

Fig. 1: Schematic depicting the Q-boosted optomechanical resonator (circuit) to be demonstrated via the proposed work and to include (a) a high optical Q_o, but likely low mechanical Q_M, optical resonator; (b) several non-optical resonators constructed in a material with much higher mechanical Q_M; (c) mechanical couplers to share energy between resonators and thereby raise the Q_M of the optical resonator; (d) an integrated MEMS-tunable waveguide coupler for photonic input; and (e) multiple capacitive electrodes to both sense output motional currents and tune the mechanical frequency of the structure. This device will be embedded in the feedback control loop of a chip-scale atomic clock or sensor.

Q_o) CaF_2 resonator to share mechanical energy as described in [5] towards raising the mechanical Q_M of the CaF_2 resonator by $n\times$, where n is the number of resonators coupled in the array. This then circumvents the mechanical vs. optical Q trade-off, allowing independent optimization of both towards unprecedented optomechanical performance.

2) Use of ***GHz spoke-supported ring resonators*** invented and first published by this proposing team in 2004 [6], and apparently copied now by some in the optomechanical world, who seem to be calling it a spoke-supported toroid. Beyond merely using spoke supports, our original design also utilized higher order contour modes to cancel energy to supports, together with quarter-wavelength design and notching at support attachment locations to attach more closely to nodal locations and thereby reduce losses even further. Our previous work in polysilicon achieves Q_M = 15,000 at ~1.5GHz, for a $(1/2\pi)\omega_M$-Q_M product $>2\times10^{13}$, which is more than 2 orders better than any of the examples in the BAA document. This work will utilize ***polydiamond or SiC*** as the Q-boosting mechanical resonator material, plus ***nanowire supports*** (if needed), to substantially reduce anchor losses even beyond that demonstrated in [6], all en route to tethered Q's potentially >50,000 at GHz frequencies that will greatly increase the Z of the BAA. This geometry will also maximize the Q_M of the optical resonator in Fig. 1(a), but since it will be constructed in CaF_2 or silica, its Q will still likely be much lower than the diamond or SiC ones, so must be boosted by the circuit of Fig. 1.

3) Use of an ***integrated on-chip MEMS-tunable optically-coupled input*** and a choice of either optical or ***capacitive output***, the latter of which allows for the much lower noise detection circuit possibilities offered by transistors versus photodiodes. Here, (n-1) resonators used in the array can all contribute to the capacitive output current. This effectively multiples the available output current by (n-1), hence, further boosts the signal-to-noise ratio of the detection signal.

4) Demonstration for the first time of ***light-induced damping (or anti-damping) on resonators constructed of non-optical materials***, which is essentially what happens to the diamond or SiC resonators of the mechanical circuit in the Fig. 1. In particular, the whole circuit operates with a very specific mode shape, where all resonators experience the same reduction in displacement as the optical resonator being directly damped (or anti-damped) by optical coupling.

As will be seen, all of the above innovations were successfully demonstrated over the course of this grant.

3. Motivation: Low Power Microwave Oscillator for a Chip-Scale Atomic Clock

Aside from the generic goals of realizing stable oscillators and making possible highly sensitive sensors, one of the specific original motivations for the proposed low phase noise OMO was to lower the power consumption of Chip-Scale Atomic Clocks (CSACs). At this point, it should be made clear that although the following CSAC approach was one source of motivation for this work, demonstration of the CSAC was never in the Statement of Work, as the budget for this effort was never sufficient to support such an activity, even before the budget was cut. (So no one should expect a working CSAC, here.) That said …

CSACs have recently entered the commercial market, offering in volumes less than 10 cc unprecedented long-term stability, with Allan deviations better than 10^{-11} at one hour [7]. MEMS technology is largely responsible for not only the small size of these atomic clocks, but also their ability to operate with substantially lower power consumption (~150 mW) than their conventional non-MEMS brethren. In particular, it is a MEMS-based micro-oven that keeps alkali metal atoms

in a vapor state while consuming only 5-10 mW of power, all due to a MEMS-enabled enormous thermal resistance.

Despite this already low power consumption versus conventional counterparts, there is still much room for improvement. In a typical CSAC, the micro-oven requires ~10 mW, and the control electronics another 10 mW [8]. Interestingly, it is the last major component—the microwave oscillator—that consumes much of the rest, ~100 mW. Indeed, it is a very conventional quartz-crystal-based synthesizer, with its power hungry frequency divider, that inevitably limits CSAC power consumption. Here, although replacement of the quartz oscillator by a MEMS-based oscillator offers further size reduction, it does not solve the power problem, since inevitably an output frequency near 10MHz is desired, so some form of power-hungry frequency division would still be required.

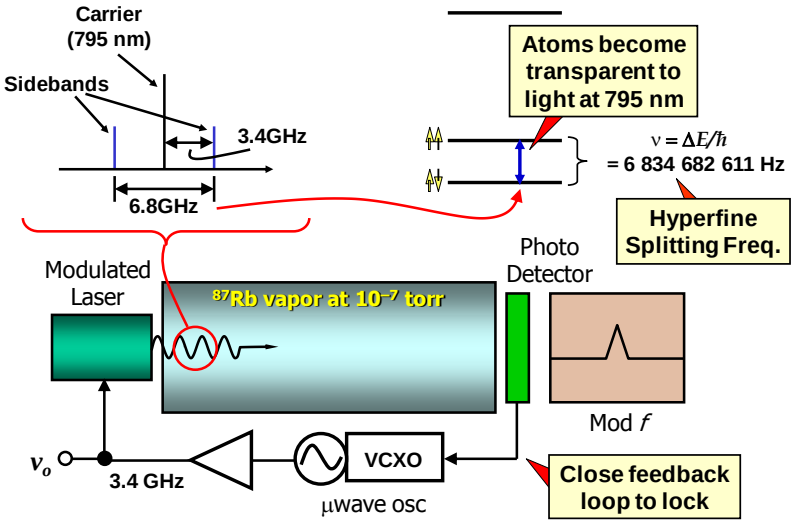

Fig. 2: Schematic describing the basic topology of a vapor cell-based atomic clock, this one exciting the hyperfine resonance via a laser-modulated approach dubbed coherent population trapping (CPT).

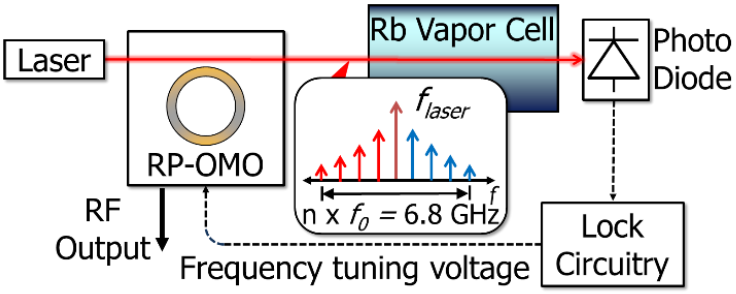

Fig. 3: Schematic of a chip-scale atomic clock topology that incorporates the proposed *Q*-boosted optomechanical resonator in place of the previous microwave oscillator of Fig. 2 to realize the same CPT locking function, but with substantially lower power consumption, as no PLL is needed.

Recognizing this, one of the goals of this work was to investigate an approach that could potentially break the power consumption barrier by dispensing with the conventional microwave synthesizer and instead replacing it with the Radiation-Pressure driven OptoMechanical Oscillator (RP-OMO) targeted by this grant. This especially given that the proposed OMO is ideally suited for applications requiring modulated optical outputs, such as CSAC, while still attaining phase noise marks commensurate with a MEMS-based oscillator without the need for frequency division.

Fig. 2 and Fig. 3, respectively, compare a conventional CPT CSAC design employing a microwave oscillator to the proposed OMO-based CSAC. As with the conventional design, the OMO-based design must deliver light to the atomic vapor cell with tones spaced by the hyperfine transition frequency. It does this by taking the laser as input, responding to the laser by mechanically oscillating at its mechanical resonance frequency, adding to the laser not only a corresponding light modulation component at the mechanical vibration frequency, but also harmonics of this frequency all the way up to the needed (for Rb) 3.4-GHz tone. Here, the two modulating tones 3.4-GHz above and below the input laser carrier frequency (or wavelength) are spaced by the needed

6.8-GHz Rb hyperfine frequency, so induce the coherent state needed for the coherent population trapping (CPT) popularly used in CSAC scale clocks.

Of course, the microwave oscillator in a conventional CSAC also generates 6.8-GHz spaced tones around a carrier light input. The power consumption difference, here, centers mainly on the need to deliver an ultimate output frequency around 10MHz, as specified by many applications. To deliver such a frequency, a microwave oscillator must divide its 3.4-GHz output down to 10MHz—a division ratio of 340 times that starts from a very high frequency—and this requires significant power consumption. The OMO, on the other hand, can be designed with a fundamental frequency of 10MHz, so might deliver the needed output frequency directly, without any need for frequency division, hence without the associated power consumption. Alternatively, it could have a frequency in the 10's of MHz, requiring only a small divide ratio many times smaller than 340, so still with practically negligible power consumption. Either way, its phase noise at the output HF frequency will be superior to that of the atomic cell and will depend strongly on the mechanical Q_m of the OMO structure, which needs to be maximized. (Thus, the concerted effort in the following pages to raise the mechanical Q_m of various OMO designs.)

However, there are issues with the proposed OMO-CSAC approach, the most unsettling of which emanates from Stark effect concerns, where the multiple harmonics generated by the OMO might induce instability via Stark effect. This is not an entirely new problem, however, as it manifests in conventional CSACs and has been solved. The difference, here, is that the extra "tones" are below and above the hyperfine frequency, rather than just above for the case of a conventional CSAC. Differences or not, there is probably a reasonable solution to the problem in the proposed OMO-CSAC, perhaps something similar to those used for conventional CSACs.

4. Accomplishments & Problems Addressed

A final report on the technical status for this grant now follows on an accomplishment-by-accomplishment basis in essentially chronological order. For each accomplishment, an objective is given, followed by a detailed account of specific accomplishments, all culminated by "next step" information with the intent of conveying what ought to be done in the future.

4.1. Optical *Q* Enhancement Via PSG Reflow

Objective: Smooth phosphosilicate glass (PSG) surfaces via anneal-based reflow of the PSG in order to enhance the optical Q_o of the material for use in OMOs.

Accomplishment: An exhaustive set of experiments have identified optimal annealing conditions to maximize the Q_o of reflowed PSG OMO spoke-supported rings like that shown in Fig. 4, which was fabricated using the process flow of Fig. 5. Table 1 presents a subset of the data taken, presenting measured optical Q_o's for PSG rings with different thicknesses and various reflow anneal time and temperature recipes. The highest measured Q_o was 6.5 million, attained by a 2μm-thick PSG ring processed with a 4-

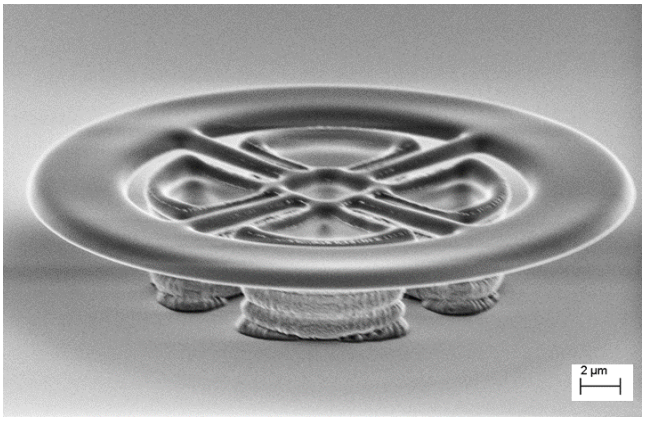

Fig. 4: SEM of a fabricated 4-spoke-supported PSG ring optomechanical oscillator (OMO).

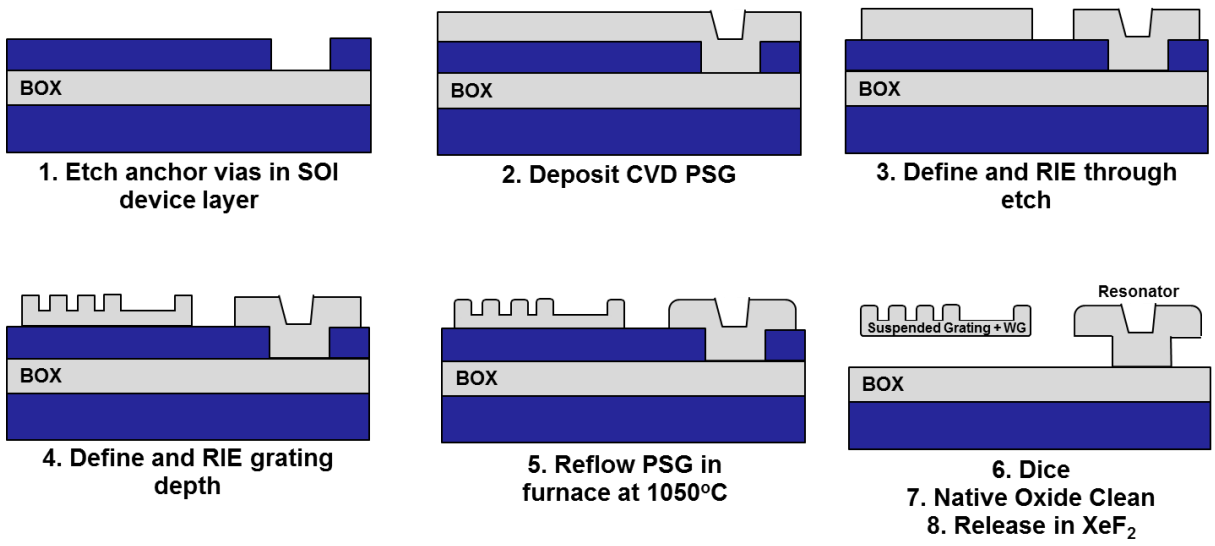

Fig. 5: Fabrication process flow used to achieve spoke-supported PSG ring OMOs.

Table 1: Summary PSG Ring Anneal Strategies to Enhance Q_o

Device Material	Material under Ring	Mask	Etch	Reflow	Best Q_{opt}
PSG, 900nm	Si_3N_4	PR	C_4F_8, H_2, He RIE	1hr @ 1050°C	1.5M
PSG, 900nm	Si	PR	C_4F_8, H_2, He RIE + HF	2hr @ 1050°C	2.1M
PSG, 900nm	Si	PR	C_4F_8, H_2, He RIE + HF	4hr @ 1050°C	2.7M
PSG, 2µm	Si	PR	C_4F_8, H_2, He RIE	1hr @ 1050°C	2.4M
PSG, 2µm	Si	PR	C_4F_8, H_2, He RIE	2hr @ 1050°C	2.7M
PSG, 2µm	Si	PR	C_4F_8, H_2, He RIE	4hr @ 1050°C	**6.5M**
PSG, 2µm	Si	PR	C_4F_8, H_2, He RIE	8hr @ 1050°C	3.2M
PSG, 2µm	Si	PR	C_4F_8, H_2, He RIE	2hr @ 1100°C	5.3M
PSG, 3µm	Si	PR	C_4F_8, H_2, He RIE	2hr @ 1050°C	~10K
PSG, 3µm	Si	PR	C_4F_8, H_2, He RIE	4hr @ 1050°C	3.0M
PSG, 3µm	Si	PR	C_4F_8, H_2, He RIE	2hr @ 1100°C	3.7M
PSG, 3µm	Si	PR	C_4F_8, H_2, He RIE	4hr @ 1100°C	3.6M

hour reflow anneal at 1050°C. For this particular device type, annealing at 1050°C for longer than 4 hours, e.g., 8 hours, actually reduced the optical Q_o, possibly due to formation of bubbles after a certain amount of time at that temperature. Other devices annealed at 1050°C also seemed to attain maximum Q_o in the 4 hour time range.

The few data points for a 3µm-thick PSG ring annealed at a higher 1100°C showed better Q_o of 3.7 million at a shorter anneal time of 2 hours, rather than 4 hours (Q_o of 3.6 million), although not by much. It's possible that the value of Q_o depends to some extent on a time-temperature product like many other semiconductor processing mechanisms. Although further quantifying this

work would be interesting and valuable, we stopped the investigation when it became clear upon further exploration that mechanical Q_m had a larger influence on OMO performance than optical Q_o.

Next Steps: As mentioned, further quantification of Q_o as a function of anneal time and temperature would be useful and perhaps will be done using data already taken and published as a journal paper in the future.

4.2. Nitride Versus PSG OMO Comparison: Lower Optical *Q* Is Better

Objective: Confirm by direct comparison of fabricated OMO's that mechanical Q_m more strongly influences the ultimate phase noise of an HF or VHF OMO than optical Q_o, and that high optical Q_o might actually be detrimental to phase noise performance.

Accomplishment: The phase noise of OMO's fabricated in reflowed PSG and silicon nitride was measured and compared under different operating pressures in order to gauge the impact of mechanical Q_m and optical Q_o. Here, pressure served as a knob for mechanical Q_m, while material type a knob for optical Q_o, where the inability to smooth etched nitride sidewall surfaces relegates OMO's using it to Q_o's on the order of 100,000 much smaller than the millions of reflowed PSG counterparts. Via these experiments, an OMO attaining an anchor-loss-limited mechanical Q_m of 10,400 in vacuum has posted a best-to-date (at the time) phase noise of -102 dBc/Hz at a 1-kHz offset from a 74-MHz carrier, which at the time was more than 15 dB better than the best previously published mark [1]. While enhanced optical and mechanical Q both serve to lower the optical threshold power required for oscillation, it is the mechanical Q_m that ends up having the strongest impact on phase noise [2], much as in a traditional MEMS-based oscillator [3]. The improved phase noise performance of this OMO was on par with many conventional MEMS-based oscillators and is sufficient for the targeted chip-scale atomic clock application.

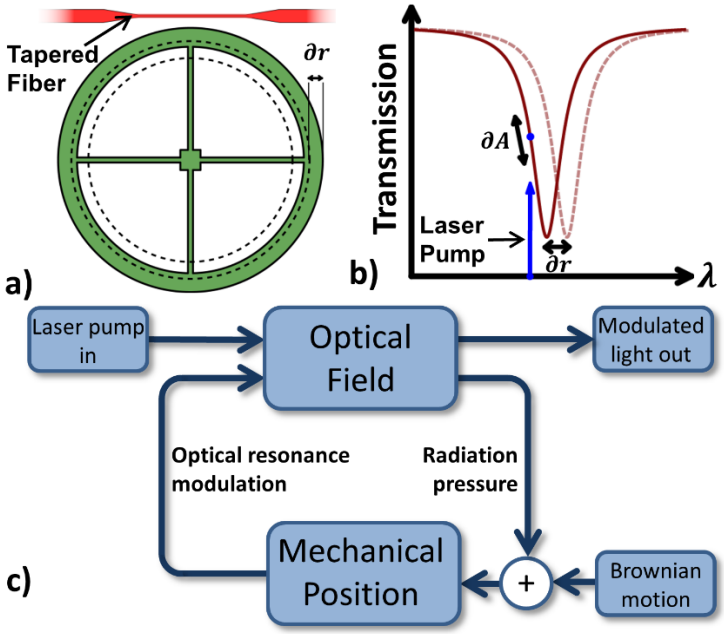

Fig. 6: Operation of an RP-OMO. As the ring resonator coupled to tapered fiber in (a) displaces by ∂r, the optical path length change produces the shift of the resonance wavelength shown in (b) and subsequently, the circulating power amplitude (and phase), ∂A. With a blue-detuned laser pump, the closed-loop feedback system of (c) is created, where the interaction of optical field and mechanical position produces laser power-dependent parametric amplification of resonator motion.

In the RP-OMO as depicted in Fig. 6, blue-detuned (i.e., with shorter wavelength than that of the optical resonance) laser light couples into the optomechanical resonator, producing a Q_o-enhanced radiation pressure force on the outside of the ring. The radiation force displaces the mechanical resonance, increasing the optical path length, and thus intrinsically coupling optical and

mechanical modes. In a process analogous to Raman scattering, photons are scattered up in wavelength by the mechanical resonance, producing a parametric amplification of the initially Brownian mechanical motion, which for sufficient optical power, generates a self-sustained oscillation of the mechanical mode. Depicted graphically in Fig. 6(c), this interaction is described by the differential equations [9]:

$$\ddot{r}(t) + \Gamma_{\mathrm{m}}\dot{r}(t) + \left(\frac{f_0}{2\pi}\right)^2 = \frac{F_{\mathrm{rp}}}{m_{\mathrm{eff}}} \tag{1}$$

$$\dot{A}(t) + A(t)\left[\gamma_{\mathrm{tot}} - i\Delta\omega + i\frac{\omega_0}{r_{\mathrm{o}}}r(t)\right] = iB\sqrt{\frac{2\pi r_o}{c}\gamma_{\mathrm{ext}}} \tag{2}$$

where $r(t)$ is the radial displacement of the mechanical resonator from equilibrium, Γ_{m} is mechanical damping, $\omega_{\mathrm{m}} = 2\pi f_0$ is mechanical resonance frequency, $A(t)$ the optical field in the resonator, $\Delta\omega$ the detuning of laser from optical resonance frequency ω_0, B input pump laser field, γ_{tot} the total optical resonator damping, γ_{ext} the coupling between optical resonator and the tapered fiber, and m_{eff} a mode-dependent mechanical effective mass defined such that $m_{\mathrm{eff}} = 2U/(r_{\mathrm{max}}^2\,\omega_{\mathrm{m}}^2)$ with U being total energy stored in the mechanical mode. F_{rp} is the radiation pressure force produced by the circulating light, given by $F_{\mathrm{rp}} = 2\pi n P_{\mathrm{c}}/c$, where n is effective index of refraction, c is speed of light, and P_{c} is the power circulating the cavity. When driven by a laser, the RP-OMO operates as in Fig. 6, where motion of the ring shifts the optical resonance, modulating the circulating light, which in turn produces feedback in the form of radiation pressure on the mechanical mode. This interplay is similar to traditional oscillator loops with the optical field acting as a parametric amplification on mechanical motion, with the phase of the driving force dependent on the relative detuning of laser to optical resonance and the gain on the optical power. To start-up oscillation, the loop phase-shift of the feedback force must be zero. In addition, the optical power provided by the blue-detuned laser pump must be sufficient to overcome losses towards a positive loop gain.

The RP-OMO is a unique oscillator in that, in principle, the optical feedback may be shot-noise limited; however, background thermal noise still exists in the form of Brownian forces on the mechanical resonator. This noise is shaped by the parametric gain and gives rise to phase noise

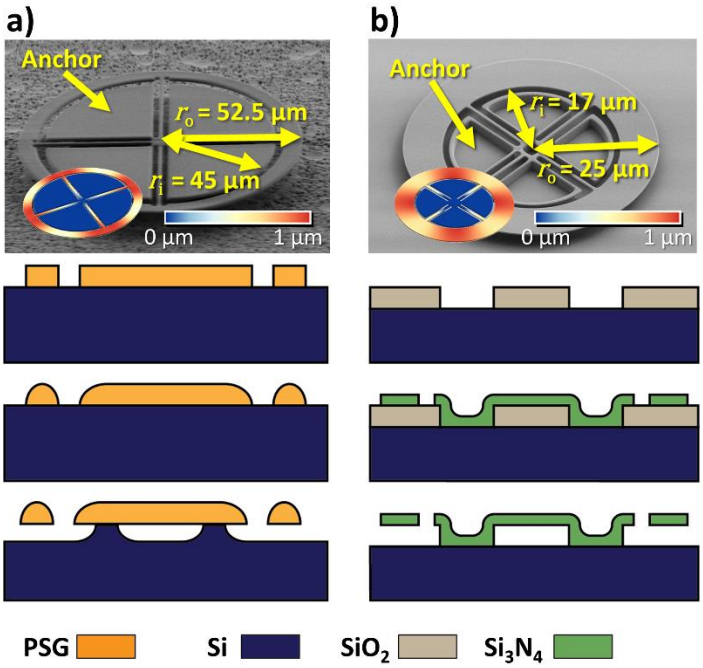

Fig. 7: SEM images and the corresponding fabrication process for (a) PSG devices consisting of LPCVD deposition of PSG, etch in C_4F_8, reflow at 1050°C, and timed release in XeF_2;, and (b) nitride devices with an added anchor etch. Nitride is etched with SF_6, and released in 10:1 BHF. Inset FEM simulations show mode shapes for the fundamental contour mode excited by the optical interaction.

in the final output oscillator spectrum [10]. While the mechanics of amplification and oscillation in the RP-OMO are novel, as with any oscillator the phase noise may be understood in the context of regenerative amplification of thermal noise, shaped by the tank-circuit feedback element [11]. Such a treatment gives rise to the well-known Leeson's equation for phase noise [12]:

$$\mathcal{L}(f) \cong 10 \log\left[\frac{2FkT}{P_{\text{sig}}}\left(1+\frac{1}{Q^2}\left(\frac{f_o}{2\Delta f}\right)^2\right)\right] \quad (3)$$

where $\mathcal{L}(f)$ is the single side-band phase noise at an offset Δf from carrier of an oscillator operating with output power P_{sig} and a tank-circuit element with quality factor Q: in this case the mechanical quality factor. Noise factor F expresses the total additive noise in the system and is a function of intrinsic Brownian noise and any additive laser noise. Compared with traditional electronic oscillators, P_{sig} is complicated to measure, but may be calculated as a numerical solution to the coupled differential equations as in [10]. While improvements may be made to P_{sig}, the strong Q_m^2 dependence motivates a primary focus on improving Q_m for decreased phase noise.

Fig. 7 presents SEMs and fabrication processes of ring-shaped RP-OMOs made in two materials: phosphosilicate glass (PSG) with modest Q_m and high Q_o; and stoichiometric silicon-nitride with low Q_o but high Q_m. Fabrication for these devices comprise one or two-mask wafer-scale processes with an added reflow step for PSG devices [13] that enable Q_o's of 6.5million—a marked improvement over previous state-of-the-art one-by-one laser-annealed devices [14]. Since they do not benefit from a similar such smoothing process, nitride devices are generally limited to Q_o's around 100,000.

Optical interrogation of fabricated devices in vacuum demanded construction of the custom vacuum probe system shown in Fig. 8, which provides both optical and electrical interrogation and measurement. Here, light couples in and out of the on-chip RP-OMO via a tapered fiber [15] mounted on a specially-designed three-axis nano-positioning stage. With 10

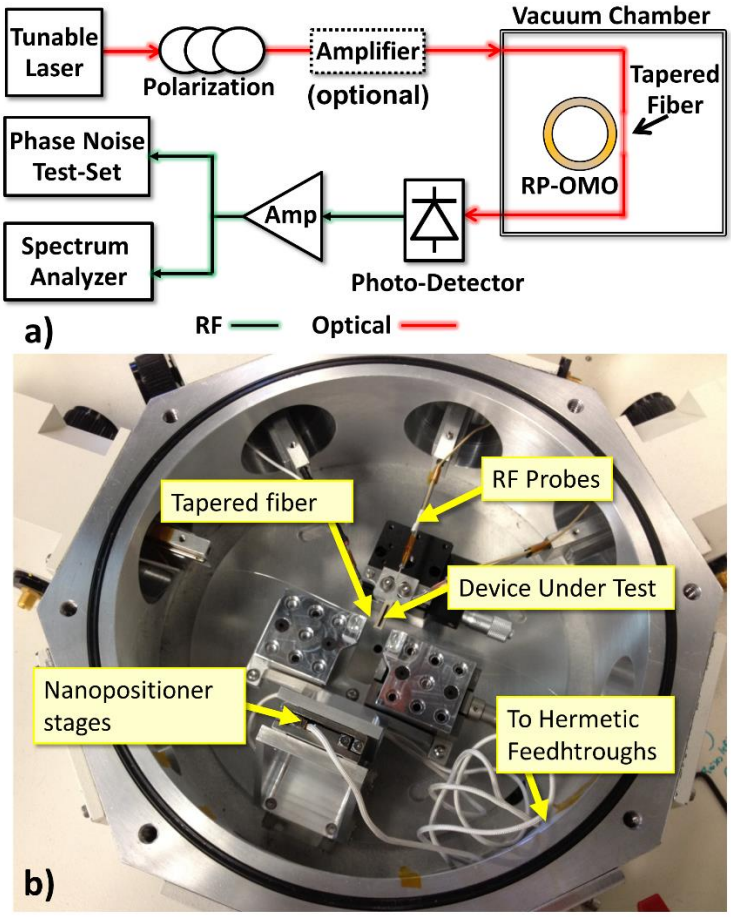

Fig. 8: Experimental measurement setup consisting of (a) the measurement circuit comprised of a Newfocus TLB-6728 tunable laser, optional Erbium-doped fiber amplifier and photo-diode amplifier chain feeding an Agilent N9030A spectrum analyzer and a E5505A phase noise test system; and (b) the custom-built vacuum chamber including tapered-fiber, RF probes and Attocube ECS3040/NUM positioner stages with 10 nm precision.

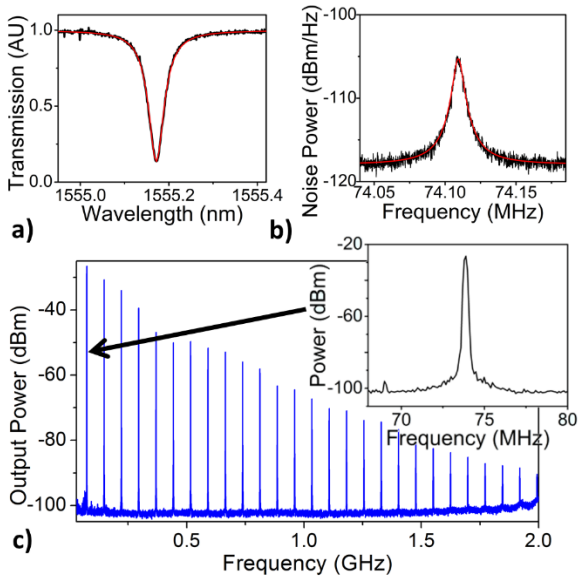

Fig. 9: Measurements of an RP-OMO showing a) an over-coupled optical resonance, b) Brownian motion of a nitride ring measured with low optical power to obtain Q_m=10,400, and c) a typical frequency comb produced by an oscillating RP-OMO.

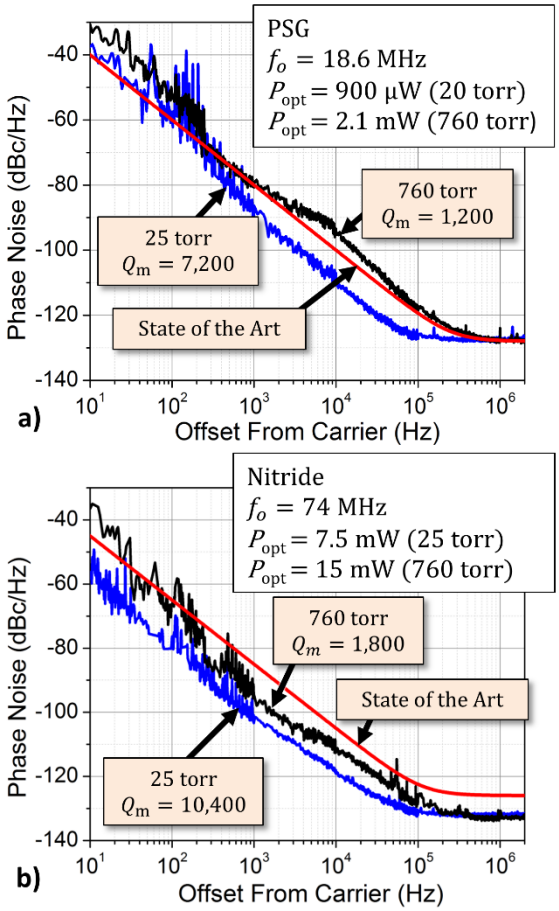

Fig. 10: Measured phase noise of (a) the 18.6-MHz PSG and (b) the 74-MHz silicon-nitride optomechanical oscillators in air (black) and vacuum (blue). For both devices, measurement in a vacuum environment removes air-damping losses, enhancing Q_m closer to device limits. The red curves represent best-to-date published phase noise data for silica [2] and nitride [1] RP-OMOs, scaled by carrier frequency.

nm repeatable precision, this system allows accurate coupling and interrogation of RP-OMO devices.

Fig. 9 presents measurements made on a nitride RP-OMO, exhibiting the typical Lorentzian curves of the optical (Fig. 9(a)) and mechanical (Fig. 9(b)) resonances from which Q_o and Q_m are extracted. Fig. 9(c) provides a first demonstration of the harmonic comb effect desired for the CSAC applications, producing sizable oscillation peaks to above 2 GHz.

Fig. 10(a) presents measured phase noise data for an 18.6-MHz PSG RP-OMO, where the phase noise in vacuum is seen to be an impressive 7-9 dB better than in air, achieving -87 dBc/Hz at a 1 kHz offset—better performance than any similar silica-based device posted to date at the time of this work. Besting even this, Fig. 10(b) shows similar curves for a 74-MHz nitride RP-OMO, yielding a similar 8 dB improvement in vacuum and posting a remarkable -102 dBc/Hz at 1 kHz offset. This improvement in phase noise closely follows that predicted by Eq. (3) for the measured Q_m-enhancement in vacuum.

A much more detailed account of this work is given in reference [4]: T. O. Rocheleau, A. J. Grine, K. E. Grutter, R. A. Schneider, N. Quack, M. C. Wu and C. T.-C. Nguyen, "Enhancement of mechanical Q for low phase noise optomechanical oscillators," in *2013 IEEE 26th Int. Conf. on Micro Electro Mechanical Systems (MEMS)*, Taipei, Taiwan, Jan. 20-24, 2013, pp. 118-121.

Next Steps: The logical next steps entail increasing the mechanical Q_m towards even better phase noise performance. This in fact is what happened over the grant, as will be described in succeeding

sections.

4.3. Co-Planar Silicon-Nitride *Q*-Boosted OMO

Objective: Lower the phase noise of optomechanical oscillators by increasing the mechanical-*Q* via coupled array-based *Q*-boosting and incorporate electrodes to facilitate electrical output and electrical frequency tuning, all using a silicon-compatible batch fabrication process.

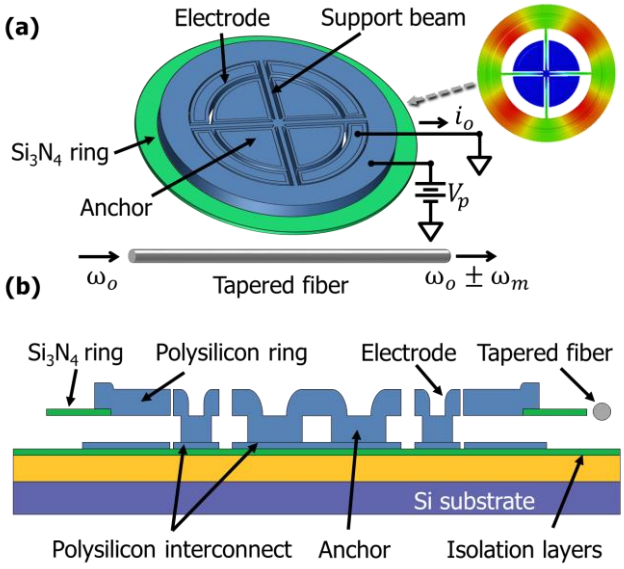

Figure 11: a) Perspective-view and (b) cross-sectional schematics of the Q-boosted RP-OMO. Here, the polysilicon inner ring is mechanically coupled at its outer edge to a concentric high optical Q_o silicon nitride ring. A tapered fiber provides optical coupling, while polysilicon electrodes inside the ring enable frequency tuning and electrical input-output.

Accomplishment: A co-planar OMO comprised of attached concentric rings of polysilicon and silicon nitride has achieved a first demonstration of a mixed material optomechanical device, posting a Q_m of 22,300 at 52 MHz, which is more than 2× larger than previous single-material silicon nitride devices [4]. With this Q_m, the OMO exhibits a best-to-date phase noise of -114 dBc/Hz at 1 kHz offset from its 52-MHz carrier—a 12 dB improvement from the previous best by an OMO constructed of silicon nitride alone [4]. The key to achieving this performance is the unique mechanical *Q*-boosting design where most of the vibrational energy is stored by the high-Q_m polysilicon inner ring which in turn boosts the over-all mechanical Q_m over that of silicon nitride, all while retaining the high optical Q_o > 190,000 of silicon nitride material.

The *Q*-boosted OMO, summarized in perspective-view and cross-section in Figure 11, comprises a high mechanical Q_m polysilicon inner ring physically attached at its outer edge to a concentric high optical Q_o (but comparatively low mechanical Q_m) silicon nitride ring. Spokes attached to the inner edges of the polysilicon ring extend radially inwards to a common central anchor and serve to support the entire multi-ring device in a completely balanced fashion, where inward forces along the spokes are met with equal and opposite ones, cancelling energy leakage from the spokes to the substrate. Polysilicon electrodes inside the ring overlap its inner edge to form capacitive gaps that then allow electrical interrogation and control (in addition to optical).

The doped polysilicon mechanical structure and inner capacitive gap electrodes are anchored and electrically connected to a thin layer of conductive polysilicon patterned on the substrate to serve as interconnects that facilitate electrical interrogation and read-out. The addition of polysilicon further provides a mechanism for voltage-controlled electrical stiffness tuning of the oscillation frequency—a necessary capability for the target chip-scale atomic clock (CSAC) application, where the OMO locks to an atomic resonance to borrow its long-term stability while providing an electrical output with excellent short-term stability.

Figure 12(a) and (b) present measured Brownian noise and optical transmission spectra of OMO showing mechanical and optical resonances and revealing a Q_o of 193,000 and boosted Q_m of 22,300, the latter more than 2× higher than demonstrated in a previous silicon nitride OMO.

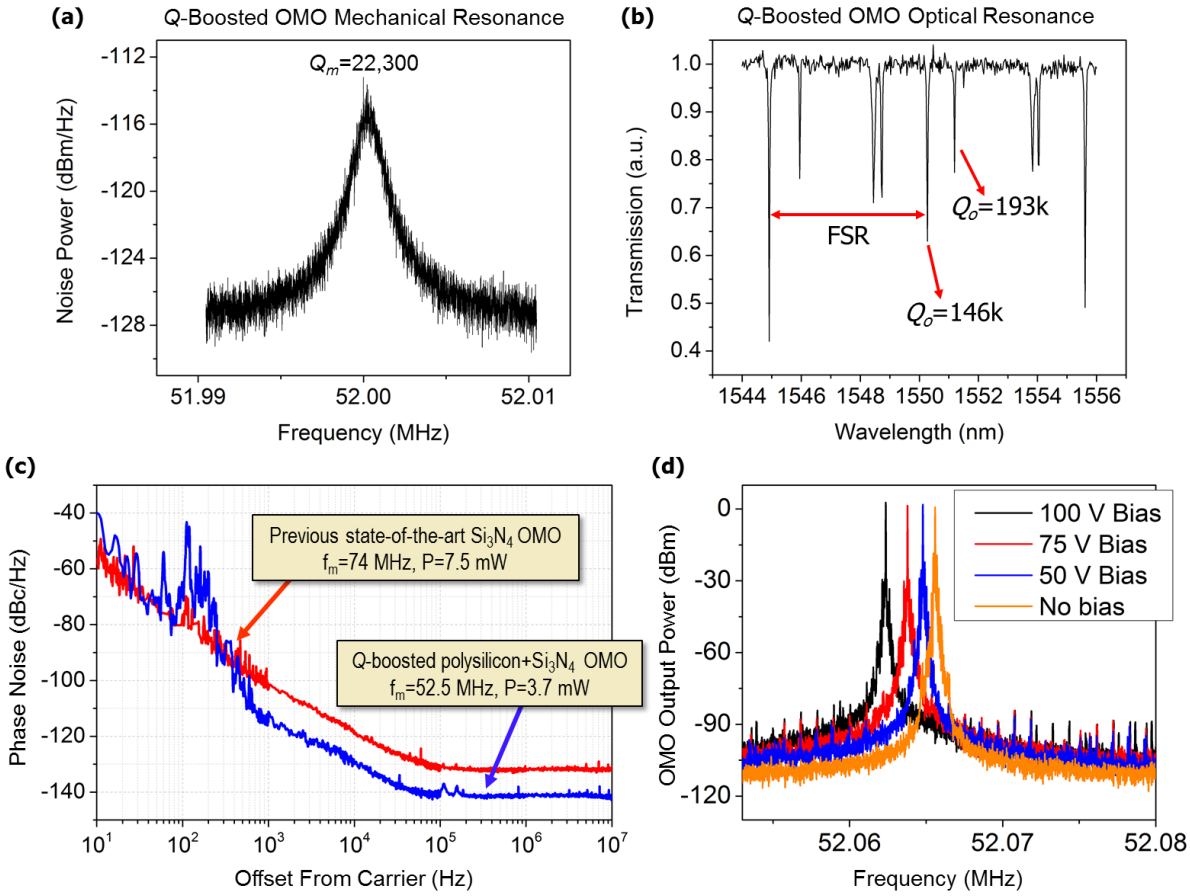

Figure 12: Measured Brownian motion (a) and optical transmission (b) of the OMO from which Q_m = 22,300 and Q_o = 193,000 are extracted. (c) Phase noise spectra of the *Q*-boosted OMO compared to the previous best Si_3N_4-only OMO [2]. As expected, the enhanced Q_m lowers the phase noise, achieving a 12 dB improvement at 1 kHz offset. (d) OMO output under several bias voltages demonstrate voltage-controlled frequency tuning.

Figure 12(c) presents the measured phase noise for the *Q*-boosted OMO of -114 dBc/Hz at 1 kHz offset from its 52-MHz carrier, which is 12 dB better than the previous state of the art OMO constructed of silicon nitride alone [4], despite the use of an input laser power of only 3.6 mW—more than 2× smaller than that of the previous state-of-the-art [4] as a result of simultaneous high Q_o and Q_m that reduces the optical threshold power for oscillation.

Figure 12(d) shows the OMO output spectra under several tuning voltages and measured plots gauging oscillating OMO frequency versus tuning voltage, where a relatively large 440 nm electrode-to-resonator gap spacing still allows a 3 ppm/V frequency shift suitable for locking to the Rb vapor cell in a CSAC.

A much more detailed account of this work is given in reference [16]: T. Beyazoglu, T.O. Rocheleau, K. E. Grutter, A.J. Grine, M. C. Wu and C. T.-C. Nguyen, "A multi-material *Q*-boosted low phase noise optomechanical oscillator," in *Proceedings, 2014 IEEE Int. Conference on MEMS*, San Francisoc, USA, Jan 26-30, 2014, pp. 1193-1196.

Next Steps: Should there have been available funding, the next step would have been to lower the

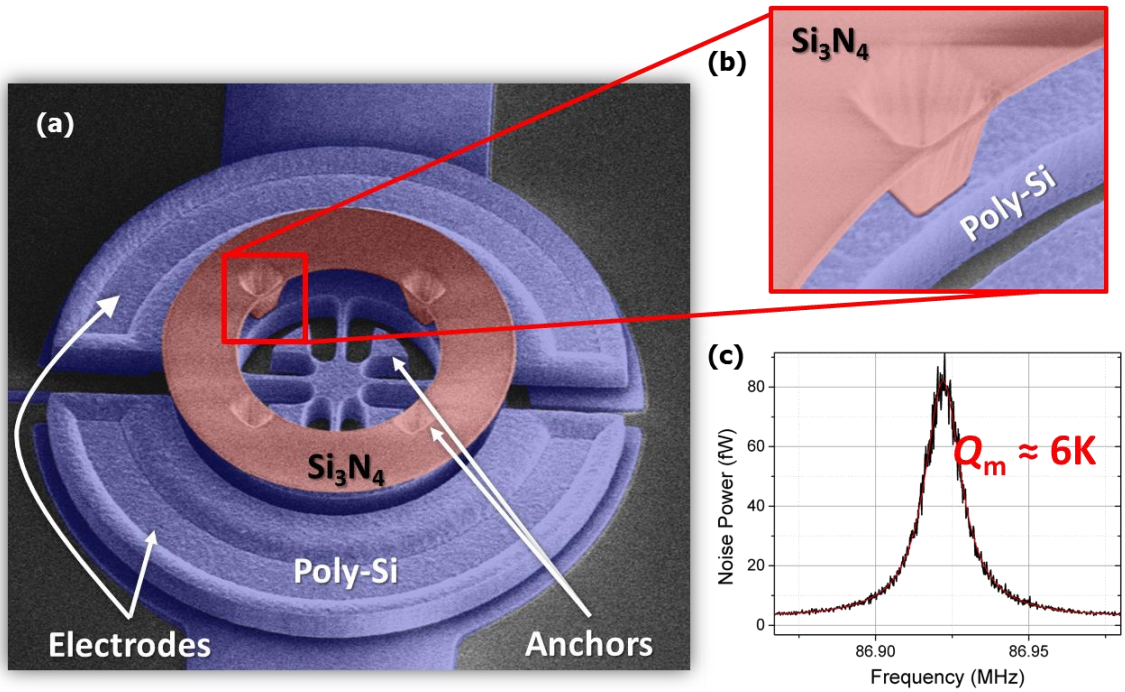

Figure 13: (a) Colored SEM image of the stacked-ring OMO with polysilicon (purple) and silicon nitride (red) layers. (b) A zoom-in on the vertical coupling beam that mechanically couples the two rings. (c) Measured Brownian noise spectrum showing a 87 MHz resonance with a Q_m = 6,000.

voltage required to tune the oscillation frequency by reducing the electrode-to-resonator gap spacing. This actually has already been done as the next section describes.

4.4. Nitride Over Silicon *Q*-Boosted OMO

Objective: Lower the phase noise of Opto-Mechanical Oscillators (OMO) and incorporate electrodes to facilitate electrical output and electrical frequency tuning. Achieve small electrode-to-resonator gap spacing using a reliable wafer-level process similar to previously demonstrated MEMS resonators [3].

Accomplishment: A multi-material composite OMO comprised of a silicon nitride ring stacked atop a polysilicon ring in a vertically coupled fashion realized a first demonstration of a 3-D opto-mechanical device, allowing independent optimization of optical and mechanical properties as well as electromechanical coupling. The first rendition of this device, with lithographically defined electrode gap requiring a simpler fabrication but sacrificing electromechanical coupling, realized an 87 MHz OMO with a threshold power below one mW. Figure 13 presents a colored SEM image of the stacked-ring OMO where the purple layer shows the polysilicon ring and surrounding electrodes and red shows the silicon nitride ring atop. A zoom-in on this image (b) reveals the vertical coupling between the nitride and polysilicon. This coupling scheme ensures that the optical field stored in the silicon nitride cavity is not affected by the mechanical coupling, which in turn allows retention of high optical-*Q* (Q_o). As such, the composite device exhibits Q_o > 154,000 similar to a silicon nitride-only cavity. The vertical coupling further allows optimized electrode placing around the device since the cavity (hence the optical field) is far above from the optically lossy polysilicon layer.

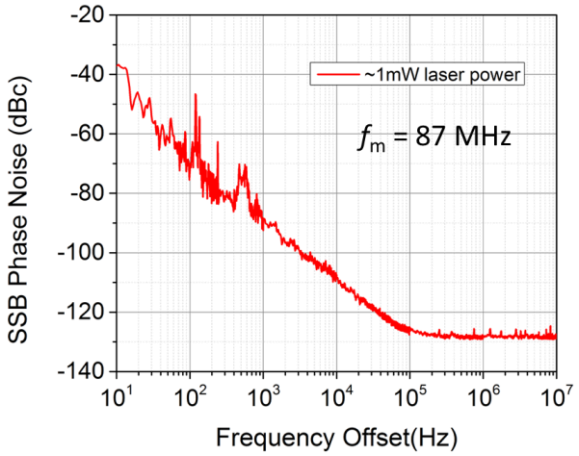

Figure 14: Measured phase noise spectra of the stacked-ring OMO with an input power of only 1 mW.

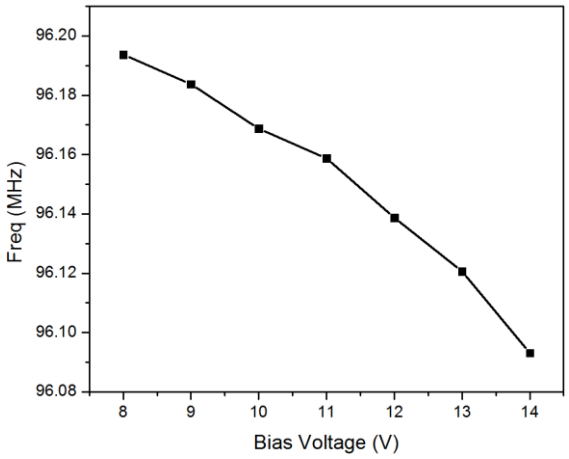

Figure 15: Stacked-ring resonance frequency under several bias voltages, demonstrating 20 ppm/V frequency shift and revealing 40 nm gap spacing.

Figure 14 presents the measured phase noise of the stacked-ring OMO, which, although adequately low for many applications, isn't as good as the phase noise performance of the co-planar *Q*-boosted OMO described in the previous section. The device rather exhibits a lower mechanical-*Q* (Q_m) of 6,000 (Figure 13(c)) which limits the phase noise performance. The most probable culprit is the unexpectedly low-Q_m polysilicon deposited in an unlucky process run in our university laboratory.

The second rendition of the stacked-ring OMO uses a process similar to previously demonstrated MEMS resonators [3], which allows definition of the electrode gap spacing by the sacrificial layer thickness that then allows much smaller gap and much stronger electromechanical coupling. The addition of the silicon nitride ring and the associated vertical couplers above the polysilicon MEMS structure requires only 2 more lithography steps atop a fairly mature and standard process flow. Figure 15 presents measured resonance frequency as a function of bias voltage V_P for one such device, yielding a curve consistent with the deposited sacrificial layer thickness of 40 nm. The observed frequency shift is almost 20 ppm/V, to be compared to the 3 ppm/V of the co-planar OMO.

Next Steps: The next step, should there have been left over funding, would have been to investigate the issues that lead to lower Q_m and iterate the device design, possibly fabricating larger arrays to raise the Q_m to that of polysilicon and allow much larger electromechanical coupling.

4.5. Lock to High Frequency Comb for CSAC

Objective: Demonstrate phase-locking using a high-order harmonic of an optomechanical oscillator to a stable microwave source in order to improve the long term stability. Basically, this mimics locking to a Rb reference in the target CSAC application.

Accomplishment: Phase-locking an Optomechanical Voltage Controlled Oscillator (OMVCO), realized by the co-planar device of the previous section, to a microwave source greatly improves the OMVCO's long term drift while simultaneously retaining its excellent short term characteristics. Phase-locking the 9th harmonic of a OMVCO at 466 MHz to an RF signal generator improved the phase noise by 85 dB at 1 Hz offset, while maintaining a phase noise of -140 dBc/Hz at offsets >50 kHz; yielding a reduction in Allan deviation by 20 dB.

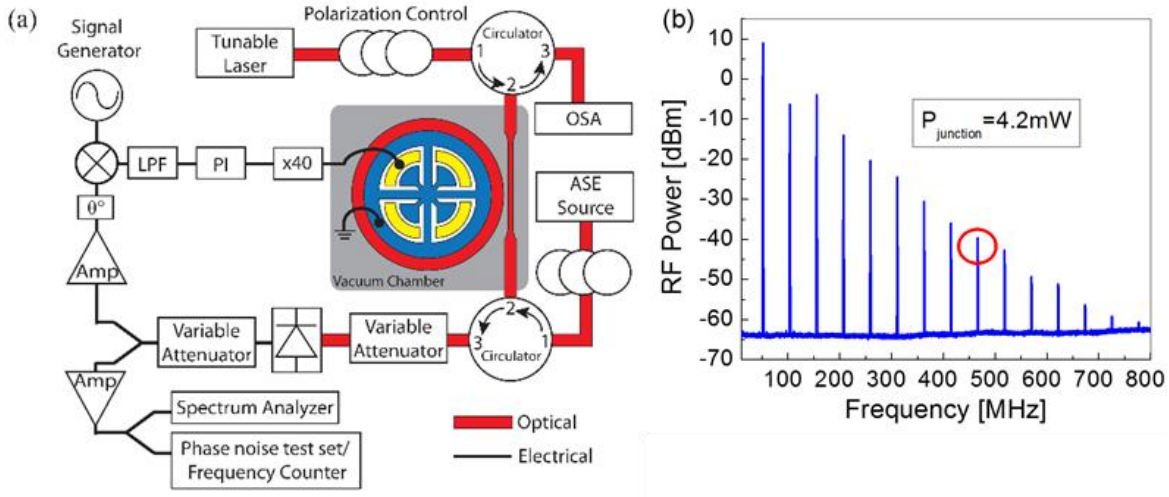

Figure 16: (a) Measurement setup for phase-locking the OMVCO 9th harmonic to an RF signal generator. Tunable laser light in the tapered fiber couples to the device and instigates self-oscillation. Light exiting the fiber is mixed with an RF signal generator, filtered and fed back to tuning electrodes. An Optical Spectrum Analyzer (OSA) simultaneously monitors transmitted light from a broadband Amplified Spontaneous Emission (ASE) source to maintain the optical coupling. LPF= Low Pass Filter. PI= Proportional Integral controller. (b) Photodetected OMVCO frequency comb viewed on the electrical spectrum analyzer after amplification. Red circle indicates 9th harmonic used for locking.

Owing to its low phase noise and voltage tunable frequency, the *Q*-boosted OMVCO is an excellent candidate for locking to a microwave reference and the eventual CSAC application. The phase noise of the locked OMVCO at small frequency offset benefits from the long term stability of the lock reference. However, the effective lock bandwidth is limited and at large offset frequencies the locked system will inevitably retain the phase noise of the free running OMO. In fact, unlike a high quality signal generator, the hyperfine transition frequency stability is poor at short time scales so the effective CSAC lock bandwidth is intentionally kept small. Thus, whether locking to a signal generator or atomic transition, it is imperative that the OMO exhibits low phase noise at large offset frequencies. The *Q*-boosted OMVCO posts phase noise of -140dBc/Hz at greater than 50 kHz offset, a 20 dB improvement over a previous harmonic lock demonstration [17]. Also, voltage controlled tuning eliminates the need for a separate intensity modulator and allows the detuning and input power to be targeted for optimal phase noise, threshold power, or harmonic generation.

Figure 16(a) presents the setup used for harmonically locking the OMVCO to a low noise reference by mixing photodetected light at the cavity output with an RF signal generator set near the ninth harmonic frequency of 466 MHz. Figure 16(b) shows the optomechanically generated frequency comb when pumped with 4.2 mW (~2.5x threshold) at the fiber-device coupling junction where up to 14 harmonics are visible. The frequency comb imprinted on the photodetector output then mixes with a low noise SRS SG384 RF signal generator. After a low pass filter, the error signal, proportional to the difference in phase between the OMVCO 9th harmonic and the signal generator, is further filtered by an SRS SIM960 proportional-integral (PI) controller followed by a 40× high voltage amplifier. The final control voltage then feeds the device tuning electrodes to tune the oscillation frequency. Variable optical and RF attenuators prevent saturation of the photodetector and RF amplifiers respectively ensuring harmonics are only created through

optomechanical transduction. The described test setup is similar to a typical Pound-Drever-Hall scheme for locking a laser to an optical cavity [18] except the OMVCO acts in place of a phase modulator and the error signal is fed back to OMVCO tuning electrodes rather than the tunable laser.

Figure 17(a) shows the measured phase noise of the (blue) unlocked vs. (red) locked OMVCO which shows an 85 dB improvement at 1 Hz offset. In addition to reduced phase noise, it is important to verify that the long term frequency drift of the locked OMVCO emulates that of the microwave reference. Figure 17(b) shows the OMVCO instantaneous output frequency subtracted by the average frequency over the ten minute span, for the open loop (black) and closed loop (red) cases. When unlocked, the OMVCO displays a maximum frequency deviation of ~10Hz over the 10 minute span. Once locked, the frequency drift improves dramatically and exhibits deviation of 150 mHz from the average. The most common measure of frequency stability is the Allan deviation which is plotted in Figure 17(c) for the three oscillators in question. Once locked, the OMVCO Allan deviation reduces by over two orders of magnitude and follows that of the signal generator housing an oven-controlled crystal oscillator. Combined with the previous phase noise data, it is evident that the composite oscillator made of the OMVCO locked to an oven-controlled crystal retains the excellent long term frequency stability of the signal generator with little to no degradation in the excellent short term stability of the OMVCO.

Next Steps: The next logical step, should there have been available funding, would have been to use this approach to improving OMO stability by phase-locking to an atomic reference.

4.6. OMO-Based Optical Receiver

Objective: Demonstrate a simple OMO-based optical receiver architecture made possible by the unique multi-material OMO design that allows coupling between electrical and optical domains via mechanics.

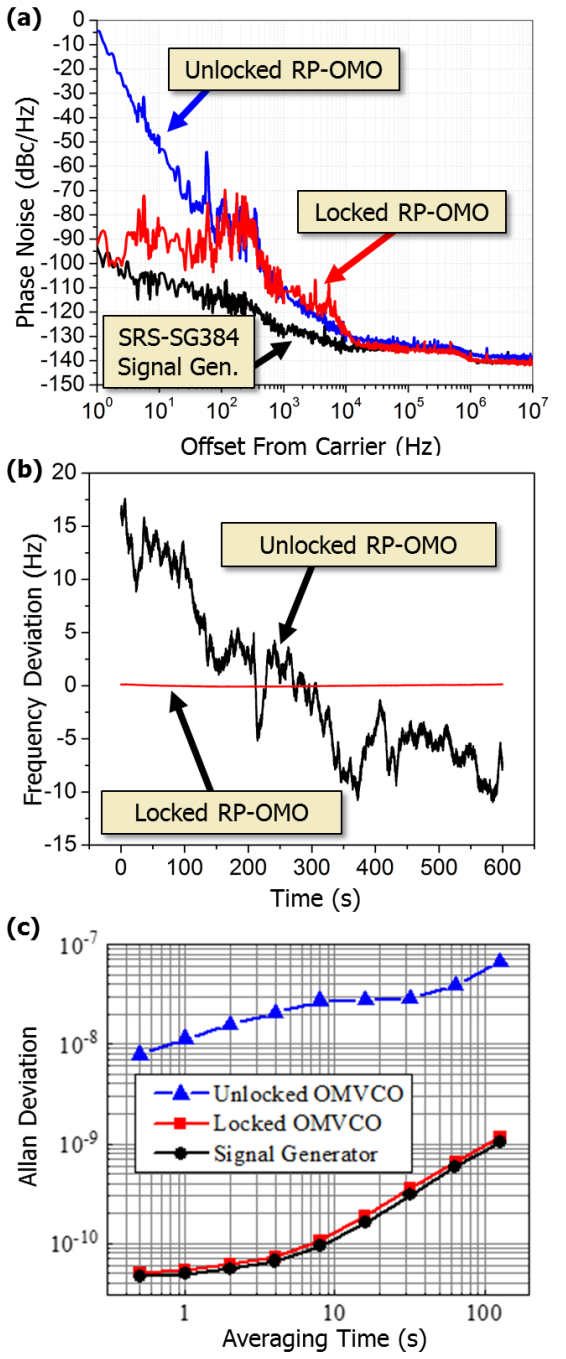

Figure 17**:** (a) Phase noise spectra of the signal generator (black) and OMVCO when unlocked (blue) vs. locked (red). Once locked, the OMVCO phase noise is suppressed by 85 dB. (b) Oscillation frequency deviation vs measurement time for the unlocked (blue) and locked (red) OMVCO. Once locked the frequency deviates by only ±150 mHz from 52 MHz compared to a ±10 Hz deviation in the unlocked case.

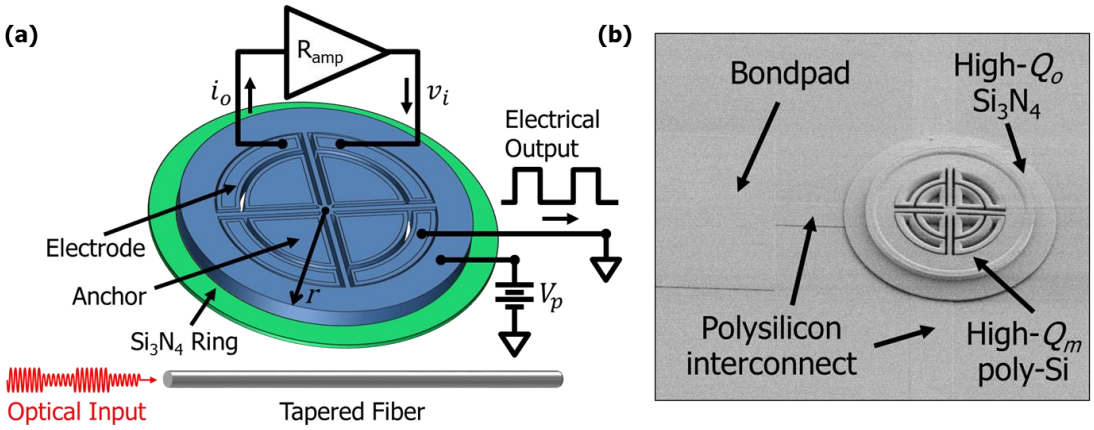

Figure 18: (a) Perspective-view schematic of the EOMO and basic receiver operation. Here, an electronic amplifier connects to input/output polysilicon electrodes and sustains oscillation. An amplitude modulated optical input couples to the Si_3N_4 ring of the EOMO and changes the output electrical oscillation amplitude, which indicates the received bits. (b) SEM image of the EOMO.

Accomplishment: The *Q*-boosted OMO has realized a first super-regenerative optical receiver that detects on-off key modulated light input via the radiation-pressure gain of a self-sustained electro-opto-mechanical oscillator (EOMO), as illustrated in Figure 18. With oscillation amplitude a function of the intensity of light coupled into the oscillator, this device now allows data to be directly demodulated using only silicon-compatible materials, i.e., without the expensive III-V compound semiconductor materials often used in conventional optical receivers.

With two I/O modes, the EOMO device of Figure 18 offers two methods to instigate self-sustained oscillation: electrical or optical. Figure 19(a) summarizes the two methods via a simple block diagram with two feedback loops. The electrical method is the same as that used in conventional oscillators, where two electrodes (i.e., capacitive-gap transducers) of the EOMO connect to the input and output terminals of an electronic amplifier to create a positive feedback loop with

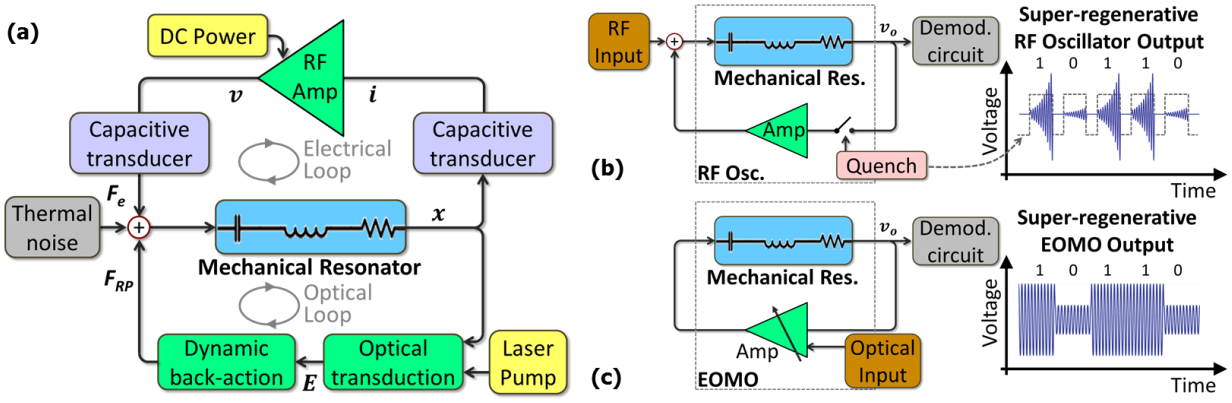

Figure 19: (a) Super-regenerative optical receiver model. Light received at the proper wavelength forms an additional positive feedback loop, thereby raising the steady-state oscillation amplitude from the no light case (where only the upper branch contributes to the loop gain). (b-c) Comparison of conventional and EOMO-based super-regenerative receivers. (b) Reception of a '1' or a '0' is determined by the speed at which oscillations reach a prescribed threshold value starting from a quenched state. (c) Reception of a '1' or a '0', without quenching, is determined by the amplitude of oscillation, which can switch quickly, greatly increasing the permissible bit data rate.

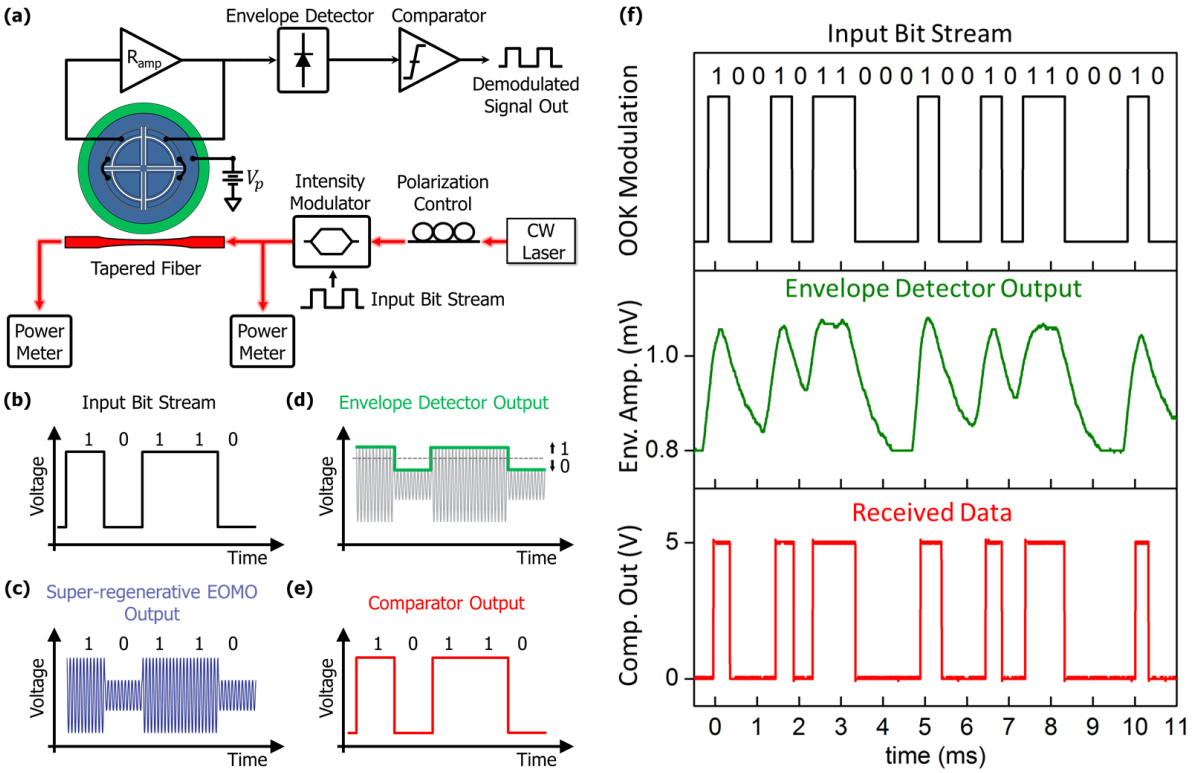

Figure 20: (a) Pictorial summary of the super-regenerative receiver. An electronic amplifier placed in a positive feedback loop with the EOMO sustains oscillation while a tapered fiber couples the optical field modulated by the input bit stream (b) into the EOMO, changing the amplitude of oscillation (c). An envelope detector measuring the amplitude (d) feeds to a comparator that recovers the data (e). (f) Measured time-traces illustrating super-regenerative optical receiver operation. (black) Input bit stream modulating a CW laser on resonance, (green) envelope detector output showing the EOMO oscillation amplitude, and (red) output bit stream for a 1 mV threshold from comparator output. The output waveform is identical to the input, as desired, confirming successful wireless optical OOK reception with a 2 kbps data rate.

loop gain greater than unity. The optical method is the same as the optomechanical gain mechanism that the OMO of a previous section utilizes. The super-regenerative optical receiver employs the gains of both Figure 19(a) modes, simultaneously. It specifically uses the electrical mode to instigate and sustain a primary oscillation, and the optical mode to influence the amplitude of the oscillation. To facilitate analysis, Figure 19(c) condenses the complexity of Figure 19(a) into a simpler equivalent block diagram that lumps the electrical and optomechanical gain mechanisms into a single amplifier controlled by the optical input. Here, the stronger the optical input, the larger the amplifier gain. The larger the amplifier gain, the larger the nonlinearity required to limit oscillation growth, and the larger the displacement amplitude needed to generate that nonlinearity. Thus, the steady-state amplitude of the oscillator becomes a direct function of the laser input power, which is the crux behind the present super-regenerative optical receiver.

Figure 19(b-c) compares a (b) conventional super-regenerative receiver with the (c) EOMO-based one of this work. As shown, both harness the positive feedback loop gain of a closed-loop oscillator to regeneratively, i.e., cycle–by-cycle, achieve an enormous front-end gain capable of detecting tiny received signals. In the former approach, reception of a ‘1’ or a ‘0’ is often determined by the speed at which oscillations reach a prescribed threshold value after starting from a quenched state, where quenching is done for every bit cycle. In this mode of operation, the bit rate

is limited by both the speed at which oscillations grow and the speed at which they can be quenched.

The EOMO-based approach of this work differs in that it does not require quenching of the oscillation, as shown in Figure 19(c). From Figure 18, the design of this receiver centers around a *Q*-boosted EOMO, comprised of concentric high mechanical Q_m polysilicon and high optical Q_o nitride rings, where unlike conventional OMOs this one can be excited both optically, via a laser coupled to the outer nitride ring; or electrically, via electrodes inside the inner polysilicon ring. With reference to Figure 20, the EOMO's electrodes are embedded in a positive feedback loop with an electronic amplifier, providing enough gain for oscillation even in the absence of an optical input. An input light that is slightly blue-detuned from the optical resonance wavelength (corresponding to a '1' in OOK) induces radiation pressure, increasing the total force (and the loop gain) applied to the mechanical resonator, and thereby raising the steady-state oscillation amplitude from the no light case (which corresponds to a '0'). The oscillation amplitude thus indicates whether a '1' or a '0' is received. Figure 20 illustrates this receiver operation by comparing time domain traces at the (c) EOMO output, (d) envelope detector, and (e) comparator outputs, for a given input bit stream (b). Here, since the oscillator merely switches between amplitude states, the time it takes for the amplitude to grow is shorter than growing from zero, so 0-to-1 transitions can be quite fast.

Figure 20(f) presents measured time-traces confirming receiver operation. Here, an input bit stream modulates the power of a CW 1550 nm laser between 13 μW, indicating a '0', and 750 μW, indicating a '1'. This modulated light input then couples to the EOMO, modulating its radiation pressure gain, thereby modulating the oscillation amplitude. The EOMO's electrical output then feeds an envelope detector that produces the envelope trace in Figure 20(f) (green). The amplitude trace is then directed to a comparator that produces the output bit stream (red) which is identical to the input stream of Figure 20(f) (black), confirming successful optical OOK reception with a 2 kbps data rate.

A much more detailed account of this work is given in reference [19]: T. Beyazoglu, T.O. Rocheleau, A.J. Grine, K. E. Grutter, M. C. Wu and C. T.-C. Nguyen, "A super-regenerative receiver based on an optomechanical oscillator," in *Proceedings, 2015 IEEE Int. Conference on MEMS*, Estoril, Portugal, Jan 18-22, 2015, pp. 976-979.

Next Steps: The next step is to incorporate the amplifier and other electronics on a chip and demonstrate a system-on-chip realization of this receiver.

5. Summary

This grant set out to prove that heterogeneous combination of multiple materials greatly improves optomechanical oscillator performance to point of permitting demonstration of actual real-world applications, such as the optical receiver that culminated this work. In this endeavor, the grant has been quite successful, as it has yielded HF to VHF optomechanical oscillators with the lowest in-class room temperature phase noise yet demonstrated. In particular, the energy sharing approach ("dubbed *Q*-boosting") combines polysilicon and silicon nitride materials to allow simultaneous high mechanical Q_m and higher optical Q_o than attainable by polysilicon material alone.

Specifically, a co-planar OMO comprised of attached concentric rings of polysilicon and silicon nitride that achieved a first demonstration of a mixed material optomechanical device, posting a Q_m of 22,300 at 52 MHz, which is more than 2× larger than previous single-material silicon nitride devices [4]. With this Q_m, the OMO exhibits a best-to-date phase noise of -114 dBc/Hz at 1 kHz offset from its 52-MHz carrier—a 12 dB improvement from the previous best by an OMO

constructed of silicon nitride alone [4]. The key to achieving this performance is the unique mechanical *Q*-boosting design where most of the vibrational energy is stored by the high-Q_m polysilicon inner ring which in turn boosts the over-all mechanical Q_m over that of silicon nitride, all while retaining the high optical Q_o > 190,000 of silicon nitride material.

As originally proposed, combination of polysilicon and silicon nitride materials in this fashion not only boosts the effective mechanical Q_m several times over that of silicon nitride alone, it also provides an ability to interrogate the device electrically (in addition to optically) via electrodes spaced very close to the OMO polysilicon ring edges. The capacitive gaps so generated enable not only electrical excitation and sensing of device motion, but also voltage-controlled tuning of its mechanical resonance frequency via electrical stiffness tuning. Using this latter effect, this effort successfully locked an optomechanical voltage-controlled oscillator (OMVCO) to a microwave source to greatly improve the OMVCO's long term drift while simultaneously retaining its excellent short term characteristics. In particular, phase-locking the 9th harmonic of a OMVCO at 466 MHz to an RF signal generator improved the phase noise by 85dB at 1 Hz offset, while maintaining a phase noise of -140 dBc/Hz at offsets >50 kHz; yielding a reduction in Allan deviation by 20 dB. Demonstration of locking in this manner simulates locking to an atomic clock output, which again, meets the goal of the original proposal (which was never to demonstrate an atomic clock, since funding was never at a level needed for this kind of goal).

Finally, embedding the capacitive-gap transducer electrodes of a co-planar polysilicon-silicon nitride OMO into a positive feedback loop with a sustaining electronic oscillator permitted demonstration of a super-regenerative optical receiver that detects on-off key modulated light input via the radiation-pressure gain of a self-sustained electro-opto-mechanical oscillator (EOMO), as illustrated in Figure 18. With oscillation amplitude a function of the intensity of light coupled into the oscillator, this device receives and demodulates incoming optical data using only silicon-compatible materials, i.e., without the expensive III-V compound semiconductor materials often used in conventional optical receivers. This demonstration constitutes an unexpected bonus result from this effort that goes well beyond what was originally proposed and that has deep ramifications for future low-power wireless communication capabilities. Perhaps the most important takeaway from this demonstration is that the optomechanical oscillator concept that started the program as merely an interesting physical phenomenon has blossomed to a technology that makes possible a silicon-compatible optical receiver.

6. References

[1] S. Tallur, S. Sridaran and S. Bhave, "A Silicon Nitride Optomechanical Oscillator with Zero Flicker Noise," in *IEEE Int. Conf. on MEMS*, Paris, 2012, pp. 19-22.

[2] A. Grine, N. Quack, K. Grutter, T. Rocheleau and e. al., "Wafer-scale silica optomechanical oscillators with low threshold power and low phase noise for monolithic optical frequency references," in *IEEE Int. Conf. on Opt. MEMS and Nanophotonics*, 2012, pp. 51-52.

[3] Y.-W. Lin, S. Lee, S.-S. Li, Y. Xie, Z. Ren and C. T.-C. Nguyen, "Series-resonant VHF micromechanical resonator reference oscillators," *IEEE J. Solid-State Circuits,* vol. 39, no. 12, pp. 2477-2491, 2004.

[4] T. O. Rocheleau, A. J. Grine, K. E. Grutter, R. A. Schneider, N. Quack, M. C. Wu and C. T.-C. Nguyen, "Enhancement of mechanical Q for low phase noise optomechanical

oscillators," in *2013 IEEE 26th Int. Conf. on Micro Electro Mechanical Systems (MEMS)*, Taipei, Taiwan, Jan. 20-24, 2013, pp. 118-121.

[5] Y.-W. Lin, L.-W. Hung, S.-S. Li, Z. Ren and C. T.-C. Nguyen, "Quality factor boosting via mechanically-coupled arraying," in *Tech. Digest, Solid-State Sensors, Actuators and Microsystems Conf. (TRANSDUCERS)*, Lyon, France, June 10-14, 2007, pp. 2453-2456.

[6] S.-S. Li, Y.-W. Lin, Y. Xie, Z. Ren, and C. T.-C. Nguyen, "Micromechanical hollow-disk ring resonators," in *Proceedings, the 17th IEEE Int. Conf. on Micro Electro Mechanical Systems*, Maastricht, The Netherlands, Jan. 25-29, 2004, pp. 821-824.

[7] "Symmetricom Product Number SA.45s Specifications".

[8] C. T.-C. Nguyen, "MEMS technology for timing and frequency control," *Ultrasonics, Ferroelectrics and Frequency Control, IEEE Transactions on*, vol. 54, no. 2, pp. 251-270, February 2007.

[9] H. Rokhsari, T. Kippenberg, T. Carmon and K. Vahala, "heoretical and experimental study of radiation pressure-induced mechanical oscillations (parametric instability) in optical microcavities," *IEEE Journal of Selected Topics in Quantum Electronics*, vol. 12, no. 1, pp. 96-107, 2006.

[10] M. Hoessein-Zadeh, H. Rokhsari, A. Hajimiri and K. Vahala, "Characterization of a radiation-pressure-driven micromechanical oscillator," *Physical Review A*, vol. 74, no. 2, p. 023813, 2006.

[11] W. Edson, "Noise in oscillators," *Proc. of the IRE*, vol. 48, pp. 1454-1466, 1960.

[12] D. Leeson, "A simple model of feedback oscillator noise spectrum," *Proceedings of the IEEE*, vol. 54, no. 2, pp. 329-330, 1966.

[13] K. Grutter, A. Grine, M. K. Kim, N. Quack, R. T., C.-C. Nguyen and M. Wu, "A Platform for On-Chip Silica Optomechanical Oscillators with Integrated Waveguides," in *Proceedings, CLEO: Sci. and Innov.*, 2012.

[14] H. Rokhsari, T. Kippenberg, T. Carmon and V. K.J., "Radiation-pressure-driven micro-mechanical oscillator," *Optics Express*, vol. 13, no. 14, pp. 5293-5301, 2005.

[15] J. Knight, G. Cheung, F. Jacques and T. Birks, "Phase-matched excitation of whispering-gallery-mode resonances by a fiber taper," *Optics Letters*, vol. 22, pp. 1129-1131, 1997.

[16] T. Beyazoglu, T. O. Rocheleau, K. E. Grutter, A. J. Grine, M. C. Wu and C. T.-C. Nguyen, "A multi-material Q-boosted low phase noise optomechanical oscillator," in *2014 IEEE Int. Micro Electro Mechanical Systems Conf.*, San Francisco, California, Jan. 26-30, 2014, pp. 210-213.

[17] J. Zheng, Y. Li, N. Goldberg, M. McDonald, X. Luan, A. Hati, M. Lu, S. Strauf, T. Zelevinsky, D. A. Howe and C. W. Wong, "Feedback and harmonic locking of slot-type optomechanical oscillators to external low-noise reference clocks," *Appl. Phys. Lett.*, vol. 102, no. 14, p. 1117, 2013.

[18] E. D. Black, "An introduction to Pound-Drever-Hall laser frequency stabilization," *Am. J. Phys.*, vol. 69, no. 1, p. 79, 2001.

[19] T. Beyazoglu, T. O. Rocheleau, A. J. Grine, K. E. Grutter, M. C. Wu and C. T.-C. Nguyen, "A super-regenerative optical receiver based on an optomechanical oscillator," in *2015 IEEE Int. Micro Electro Mechanical Systems Conf.*, Estoril, Spain, Jan. 18-22, 2015, pp. 976-979..

[20] D. Armani, T. Kippenberg, S. Spillane and K. Vahala, "Ultra-high-Q toroid microcavity on a chip," *Nature,* vol. 421, pp. 925-928, 2003.

7. List of Best Paper Award Winning Publications Resulting From This Grant

[1] T. O. Rocheleau, A. J. Grine, K. E. Grutter, R. A. Schneider, N. Quack, M. C. Wu and C. T.-C. Nguyen, "Enhancement of mechanical Q for low phase noise optomechanical oscillators," in *2013 IEEE 26th Int. Conf. on Micro Electro Mechanical Systems (MEMS)*, Taipei, Taiwan, Jan. 20-24, 2013, pp. 118-121. ***(best paper award winner)***

8. List of Publications (over the entire grant period)

[1] A. Grine, N. Quack, K. Grutter, T. Rocheleau and e. al., "Wafer-scale silica optomechanical oscillators with low threshold power and low phase noise for monolithic optical frequency references," in *IEEE Int. Conf. on Opt. MEMS and Nanophotonics*, 2012, pp. 51-52.

[2] K. Grutter, A. Grine, M. K. Kim, N. Quack, R. T., C.-C. Nguyen and M. Wu, "A Platform for On-Chip Silica Optomechanical Oscillators with Integrated Waveguides," in *Proceedings*, *CLEO: Sci. and Innov*., 2012.

[3] T. O. Rocheleau, A. J. Grine, K. E. Grutter, R. A. Schneider, N. Quack, M. C. Wu and C. T.-C. Nguyen, "Enhancement of mechanical Q for low phase noise optomechanical oscillators," in *2013 IEEE 26th Int. Conf. on Micro Electro Mechanical Systems (MEMS)*, Taipei, Taiwan, Jan. 20-24, 2013, pp. 118-121.

[4] T. Beyazoglu, T. O. Rocheleau, K. E. Grutter, A. J. Grine, M. C. Wu and C. T.-C. Nguyen, "A multi-material Q-boosted low phase noise optomechanical oscillator," in *2014 IEEE Int. Micro Electro Mechanical Systems Conf.,* San Francisco, California, Jan. 26-30, 2014, pp. 210-213.

[5] T. Beyazoglu, T. O. Rocheleau, A. J. Grine, K. E. Grutter, M. C. Wu and C. T.-C. Nguyen, "A super-regenerative optical receiver based on an optomechanical oscillator," in *2015 IEEE Int. Micro Electro Mechanical Systems Conf.*, Estoril, Spain, Jan. 18-22, 2015, pp. 976-979..

1.

1. Report Type

Final Report

Primary Contact E-mail

Contact email if there is a problem with the report.

ctnguyen@berkeley.edu

Primary Contact Phone Number

Contact phone number if there is a problem with the report

5106426251

Organization / Institution name

Dept. of EECS / University of California at Berkeley

Grant/Contract Title

The full title of the funded effort.

Q-Boosted Optomechanical Resonators

Grant/Contract Number

AFOSR assigned control number. It must begin with "FA9550" or "F49620" or "FA2386".

FA9550-10-1-0293

Principal Investigator Name

The full name of the principal investigator on the grant or contract.

Clark T.-C. Nguyen

Program Manager

The AFOSR Program Manager currently assigned to the award

Tatjana Curic

Reporting Period Start Date

07/01/2010

Reporting Period End Date

06/30/2015

Abstract

This grant set out to prove that heterogeneous combination of multiple materials greatly im-proves optomechanical oscillator performance to point of permitting demonstration of actual re-al-world applications, such as the optical receiver that culminated this work. In this endeavor, the grant has been quite successful, as it has yielded HF to VHF optomechanical oscillators with the lowest in-class room temperature phase noise yet demonstrated. In particular, the energy sharing approach (“dubbed Q-boosting”) combines polysilicon and silicon nitride materials to allow simultaneous high mechanical Qm and higher optical Qo than attainable by polysilicon material alone.

Distribution Statement

This is block 12 on the SF298 form.

Distribution A - Approved for Public Release

Explanation for Distribution Statement

If this is not approved for public release, please provide a short explanation. E.g., contains proprietary information.

SF298 Form

Please attach your SF298 form. A blank SF298 can be found here. Please do not password protect or secure the PDF

The maximum file size for an SF298 is 50MB.

completed.Nguyen UC Berkeley.AFD-070820-035.pdf

Upload the Report Document. File must be a PDF. Please do not password protect or secure the PDF . The maximum file size for the Report Document is 50MB.

150915 UCB Nguyen ORCHID FinalRpt.pdf

Upload a Report Document, if any. The maximum file size for the Report Document is 50MB.

Archival Publications (published) during reporting period:

See report.

Changes in research objectives (if any):

See report.

Change in AFOSR Program Manager, if any:

Extensions granted or milestones slipped, if any:

See report.

AFOSR LRIR Number

LRIR Title

Reporting Period

Laboratory Task Manager

Program Officer

Research Objectives

Technical Summary

Funding Summary by Cost Category (by FY, $K)

	Starting FY	FY+1	FY+2
Salary			
Equipment/Facilities			
Supplies			
Total			

Report Document

Report Document - Text Analysis

Report Document - Text Analysis

Appendix Documents

2. Thank You

E-mail user

Nov 08, 2015 20:36:26 Success: Email Sent to: ctnguyen@berkeley.edu